Vol. 09, No. 02 (2025) 10 – 18
JIIF (Jurnal Ilmu dan Inovasi Fisika)
https://jurnal.unpad.ac.id/jiif/

# CRYSTAL STRUCTURE AND OPTICAL PROPERTY OF PEROVSKITE FAPbBr3 SINGLE CRYSTALS SYNTHESIZED BY USING ANTI-SOLVENT ASSISTED VAPOR CRYSTALLIZATION METHOD

ADINDA APRILIANI NUR SUGANDI[1], AYI BAHTIAR[2*]

[1]*Undergraduate Physics Study Program, Universitas Padjadjaran*
*Jl. Raya Bandung-Sumedang Km.21 Jatinangor 45363, Sumedang, Jawa Barat, Telp. 022-7796014*
[2]*Department of Physics, Universitas Padjadjaran*
*Jl. Raya Bandung-Sumedang Km.21 Jatinangor 45363, Sumedang, Jawa Barat, Telp. 022-7796014*

**Corresponding author*
*Email: ayi.bahtiar@phys.unpad.ac.id*

Submitted: 05/02/2025
Accepted: 06/02/2025
Accepted: 06/08/2025

**Abstract**. Perovskite formamidinium lead tribromide or $FAPbBr_3$ single crystal has been intensively developed as a material for γ-ray detectors, which are very necessary in medical diagnostics in Positron Emission Tomography (PET) radio nuclear devices, in order to obtain high resolution and contrast images to accurately diagnose patient illnesses. This is because $FAPbBr_3$ has high Z, low defect density, high mobility-lifetime (μ−τ) product, is stable against γ-ray exposure, and can be synthesized in the form of large-dimensional single crystals and low-cost films. In this work, $FAPbBr_3$ single crystals were synthesized using the AVC (Anti-solvent assisted Vapor Crystallization) method. The $FAPbBr_3$ crystal has dimension of 5 mm x 5 mm x 3 mm, a single cubic crystal structure and a gap energy of 2.10 eV. The XPS results show that all bonds originating from the constituent elements of the $FAPbBr_3$ crystal are clearly observed. However, a single peak originating from O1s at 531.10 eV is clearly observed, indicating that the $FAPbBr_3$ had undergone oxidation. Optimization of the synthesis methos is needed to prevent oxygen penetration into the crystal.

**Keywords:** Perovskite, $FAPbBr_3$, single crystal, absorbance, gamma-ray detector.

***Abstrak***. *Kristal tunggal perovskite formamidinium timbal tribromida $FAPbBr_3$ telah dikembangkan secara intensif sebagai material detektor sinar-γ yang sangat dibutuhkan dalam diagnostik medis pada perangkat radionuklida Positron Emission Tomography (PET), guna memperoleh citra beresolusi tinggi dan kontras untuk mendiagnosis penyakit pasien secara akurat. Hal ini dikarenakan $FAPbBr_3$ memiliki Z tinggi, densitas cacat rendah, perkalian mobilitas-lifetime (μ−τ) tinggi, stabil terhadap paparan sinar-γ, serta dapat disintesis dalam bentuk kristal tunggal berdimensi besar dan film dengan biaya rendah. Pada penelitian ini, kristal tunggal $FAPbBr_3$ disintesis menggunakan metode AVC (Anti-solvent assisted Vapor Crystallization). Kristal $FAPbBr_3$ yang dihasilkan memiliki dimensi 5 mm x 5 mm x 3 mm, struktur kristal kubik tunggal, dan energi gap 2,10 eV. Hasil XPS menunjukkan bahwa semua*

This work is licensed under a CC Attribution 4.0 International License,
*DOI: https://doi.org/10.24198/jiif.v9i2* *e-ISSN: 2549-7014*

*ikatan yang berasal dari unsur-unsur penyusun kristal $FAPbBr_3$ dapat teramati dengan jelas. Namun, satu puncak tunggal yang berasal dari O1 pada 531,10 eV terlihat jelas, yang menunjukkan bahwa kristal $FAPbBr_3$ telah mengalami oksidasi. Optimalisasi metode sintesis diperlukan untuk mencegah penetrasi oksigen ke dalam kristal.*

***Kata kunci:*** *Perovskite, $FAPbBr_3$, kristal tunggal, absorbansi, detektor sinar-gamma.*

## 1. Introduction

Gamma-ray (γ-ray) detection using semiconductors is widely used in various fields, including medical, security, non-destructive testing of materials, nuclear plant monitoring, and archaeology. In the medical field, (γ-ray) detectors are used for medical imaging such as Positron Emission Tomography (PET) scans. High sensitivity and detection efficiency of γ-ray detector is highly needed in PET to obtain high resolution and contrast images in order to diagnose patient diseases accurately. The γ-ray detector material must have high γ-ray stopping power, large carrier charge lifetime mobility (μ–τ)**,** large resistivity to reduce noise, low defect density, and low manufacturing costs [1,2].

Currently, the γ-ray detectors that dominate the market are semiconductor-based detectors, either from single elements such as silicon (Si) and germanium (Ge), or in the form of compounds such as cadmium telluride (CdTe) [3] and gallium arsenide (GaAs) [4]. High Purity Germanium (HPGe) detectors can produce good energy resolution. This energy resolution is defined as the Full-Width-At-Half-Maximum (FWHM) of the photopeak divided by the peak centroid [5]. However, HPGe detectors have limitations, namely that they need to be cooled to cryogenic temperatures for routine operation because they have a small energy gap (0.66 eV) and low resistivity at room temperature (50 Ω cm) [6]. This causes HPGe detectors to experience very large leakage currents (which can be a source of detector noise). The need for cryogenic cooling makes HPGe detectors very expensive because they require large cooling systems and complex maintenance. Zhang & Yang (2021) made a γ-ray detector from the compound cadmium zinc telluride (CdZnTe), which does not require cryogenic cooling [7]. However, in its development, it still faces problems, namely non-uniformity of composition and high concentrations of Te inclusions. In addition, the cost of manufacturing a CdZnTe gamma-ray detector is still relatively expensive.

In the last few decades, perovskite materials, both single crystals and polycrystals (which have more grain boundaries than single crystals), have attracted widespread attention for applications in optoelectronic devices, one of which is radiation detectors. Perovskite has the chemical formula $ABX_3$ where A is $Cs^+$, MA ($CH_3NH_3^+$), FA ($CH(NH_2)_2$, Rb (MAFA), B is $Pb^{2+}$, $Sn^{2+}$, and X is Cl-, Br-, I-. The use of crystalline perovskite single radiation detector has several advantages including, a high aver-age atomic number (Z), which indicates a high stopping power for heavily charged alpha particles and a suitable mass attenuation coefficient for X-rays and γ-rays, high resistivity for reduced leakage current, high defect tolerance capability, large charge carrier mobility product (μ-τ), adjustable bandgap through tuning the halide element composition, and good thermal stability [8].

Photodetector based on the metal halide perovskite $MAPbX_3$ (X=Cl, Br, I) can produce quite good performance due to high light absorption coefficient (>105 $cm^{-1}$), variable charge carrier mobility (2.5-1000 $cm^2V^{-1}s^{-1}$), long charge carrier lifetime (0.08 - 4.5μs), and diffusion length (2-175 μm) [9]. Saidaminov et al., studied a planar integrated photodetector with a $MAPbBr_3$ single crystal which showed good performance in a

wide wavelength range [10]. The use of $MAPbBr_3$ and $MAPbI_3$ perovskites for γ-ray detectors, and found that the detectors have low noise levels and have the potential to be used for efficient and low-cost optoelectronic devices [1,11]. However, $MAPbX_3$ perovskite still has weaknesses because its chemical stability is low and tends to undergo phase transitions, making it less ideal for long-term applications such as γ-ray detectors. $MAPbX_3$ perovskite tends to be unstable under environmental conditions such as humidity, high temperature, and exposure to air. The $MA^+$ cation is an organic cation that easily decomposes when it reacts with water and oxygen, which can cause degradation of the perovskite structure. Our previous study showed that a single crystal of $MAPbBr_3$ synthesized using the ITC (Inverse Temperature Crystallization) method showed other peaks of XRD related to $PbO_2$ phases after put the $MAPbBr_3$ crystal at room temperature with high humidity, due to oxygen infiltration into the crystal [12]. Kumar et al., showed that $MAPbI_3$ underwent a thermal phase transition at relatively low temperatures [13]. At temperatures above 60°C, the structure of $MAPbI_3$ changes from tetragonal to cubic phase. To overcome the problems of chemical stability and phase transition, $MA^+$ cations can be replaced into $FA^+$ cations in lead halide perovskite. Formamidinium ($FA/HC(NH_2)_2^+$) has a cation size (2.53 Å) that is larger than the methylammonium cation ($MA/CH_3NH_3^+$) (2.17 Å), because it has more atoms. Larger cation sizes have better stability because the constituent atoms can position themselves better in the crystal lattice thereby reducing imbalances in the structure. In addition, formamidinium-based perovskite is more resistant to phase transition when heated [14]. In this work, single crystals of perovskite $FAPbBr_3$ was synthesized using AVC (Anti-solvent assisted Vapor Crystallization) method. The crystal structure, UV-Vis absorbance and bonding energy of each element of $FAPbBr_3$ crystals are presented. To the best of the knowledge of authors, no publication about $FAPbBr_3$ single crystals synthesized by the AVC method has been published. All published papers on $FAPbBr_3$ crystals were synthesized by the ITC method [15-17].

## 2. Research Methods

### *2.1. Materials*

Powder of formamidinium bromide ($CH_5N_2Br$ or MABr > 99.99%, $M_W$ = 124.97 g/mol) was purchased from Greatcell-solar materials, lead (II) bromide ($PbBr_2$ >98%, $M_W$ = 367.01 g/mol) were purchased from Merck. DMF (Dimethylformamide), and Dichloromethane (DCM) were purchased from Merck. All materials were used as received without any further purification.

### *2.2. Preparation of $FAPbBr_3$ precursor solution*

The solution was prepared by mixing FABr powder and $PbBr_2$ powder, which were then dissolved in DMF solvent. In this study, the molar ratio of FABr:$PbBr_2$ (1:1) was dissolved in DMF. The solution was then stirred using a stirrer on a hot plate at room temperature at a speed of 500 rpm for 120 minutes to obtain a homogeneous solution. The solution was then filtered using a 0.45 μm filter. The homogeneous precursor solution was put in a 5 mL vial bottle and then subjected to crystal growth using the AVC method.

### *2.3 Synthesis of $FAPbBr_3$ Crystals*

Synthesis of $FAPbBr_3$ crystals using AVC method followed the procedure used in synthesis of $MAPbBr_3$ single crystal as reported in our previous study [18]. The 2 mL vial bottle containing precursor $FAPbBr_3$ solution was placed in a bigger size bottle containing a mixture of DMF solvent and DCM anti-solvent with varied ratio. The vial

cap has a hole with a diameter of 1 mm, so that DCM can diffuse into the bottle, resulting in crystal growth. $FAPbBr_3$ crystals can grow after 7-14 days. The crystal size of $FAPbBr_3$ is affected by the mixture of DCM and DMF. If the DCM volume is too large, the crystal will grow too fast, resulting in a small crystal size. Meanwhile, if there is too small volume of DCM, the crystal will not grow. Therefore, it is necessary to optimize the ratio between the volumes of DCM and DMF to obtain $FAPbBr_3$ crystals with large dimension.

### *2.4 Characterizations of $FAPbBr_3$ Crystals*

The crystal structure of $FAPbBr_3$ crystals was determined from XRD measurement. The crystal for XRD characterization has a size of 5 mm x 5 mm x 3 mm or larger, which was obtained from 2 mL $FAPbBr_3$ precursor solution the mixture of 13 mL DCM and 7 mL DMF. The XRD pattern was measured using X-Ray Diffractometer (XRD) Bruker D8 Advance at Nano Center, Bandung Institute of Technology. The optical absorbance spectra of $FAPbBr_3$ crystals were measured using UV-visible spectrophotometer (Shimadzu UV-1800, Duisburg, Germany) at Department of Physics, Universitas Padjadjaran. The XPS (X-ray Photoelectron Spectroscopy) was conducted at The National Research and Innovation Agency (BRIN) to study the binding energy of constituent elements of perovskite $FAPbBr_3$ crystals.

## 3. Results and Discussions

### *3.1. Crystal Structure*

Measured XRD pattern of $FAPbBr_3$ crystal and COD 7130785 database are shown in Figure 1.

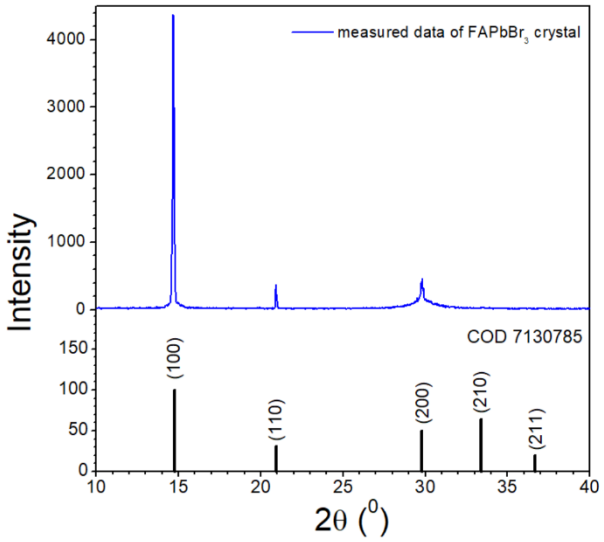


**Figure 1**. XRD pattern of $FAPbBr_3$ crystal and COD 7130785 database.

The crystal shows a domination of crystal plane oriented in the x-axis direction, indicated by the peaks (100) at 14.69° and (200) at 29.82°. However, there is a crystal plane peak (110) at 20.94° with small intensity. This result indicates that the $FAPbBr_3$ crystal is not truly single crystals, as reported by other groups [19-21]. However, our result is the same as the results of other groups who claimed that even though (110) crystal planes appear in the XRD pattern, the crystals are still called single crystals [15,16, 22]. The lattice parameter of the $FAPbBr_3$ crystal can be calculated using equation:

$$d = \frac{\lambda}{2\ sin\theta} \quad (1)$$

where d is interplanar spacing (distance between atomic planes), λ is X-ray wavelength (usually Cu Kα = 1.5406 Å) and $\theta$ is Bragg angle (half of the 2θ diffraction angle). Since $FAPbBr_3$ crystal is cubic with space group *Pm-3m* [23], the lattice parameter $a$ can be calculated using:

$$d = \frac{a}{\sqrt{h^2+k^2+\ell^2}} \quad (2)$$

where $(h\ k\ \ell)$ are the Miller indices of the crystal plane that produces the diffraction peak. rom the XRD pattern shown in Figure 1, it was found that the lattice parameter $a$ is 6.008 Å. This value is consistent with the literature report of 5.9968 Å [23].

### *3.2. UV-Vis Absorbance Spectrum*

The UV-Vis absorbance spectrum of the $FAPbBr_3$ single crystal is shown in Figure 2(a). The crystal has an absorption in the wavelength range of 500 – 590 nm. The energy gap was calculated using the Tauc plot, as shown in Figure 2(b), resulting in an energy gap ($E_g$) of 2.11 eV. This value is within the range published by other groups, which is 2.15 eV [16, 24].

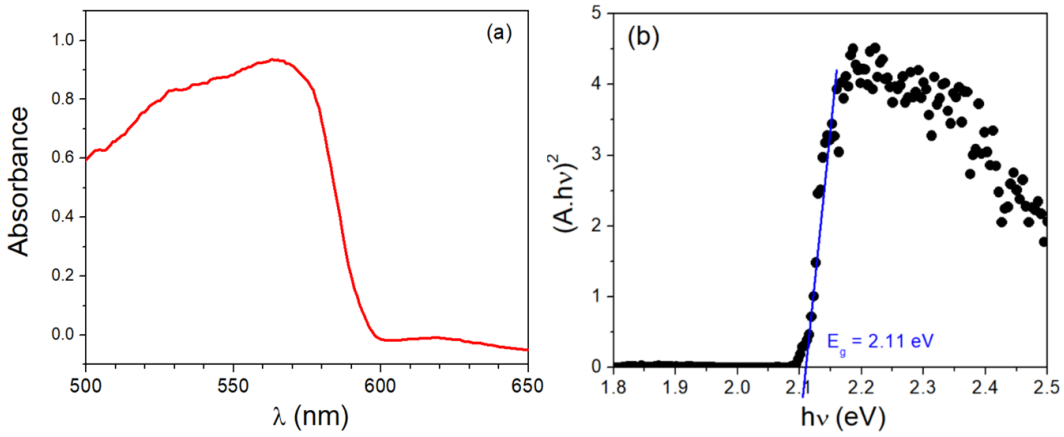


**Figure 2**. (a). UV-Vis absorbance spectrum of $FAPbBr_3$ single crystal, and (b). Tauc plot for bandgap calculation.

### *3.3. XPS Spectrum*

XPS measurement of $FAPbBr_3$ single crystals is needed to observe whether all peaks originating from all constituent elements of are detected. The XPS survey spectrum of $FAPbBr_3$ single crystal synthesized using AVC method is shown in Figure 3. The XPS spectrum is the same as reported result [25].

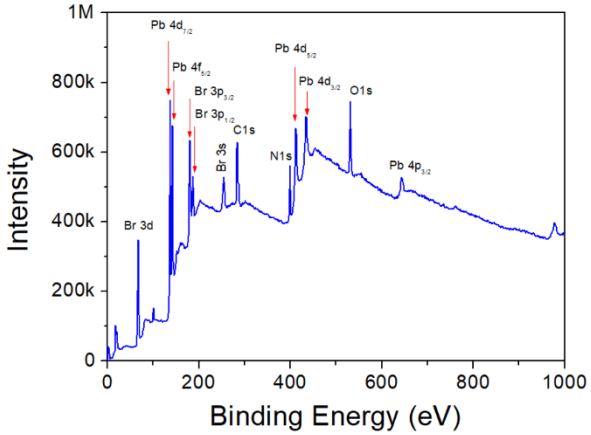


**Figure 3**. XPS survey spectrum of $FAPbBr_3$ single crystal.

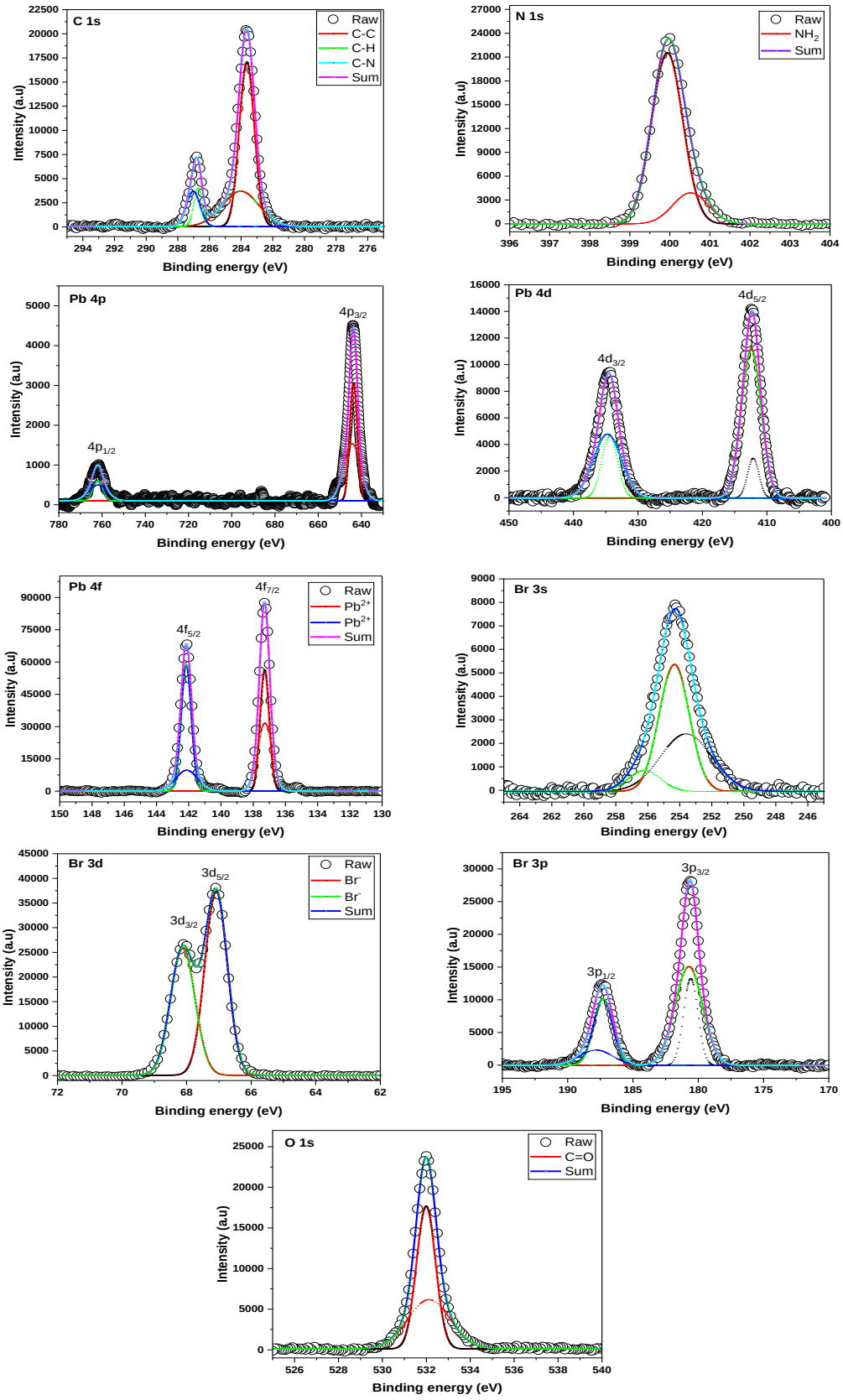


**Figure 4**. XPS spectra of each element of $FAPbBr_3$ single crystal.

To facilitate the analysis of XPS measurement results, the XPS survey spectrum is plotted in a range according to the binding energy of each constituent element, namely C, N, Pb and Br, as shown in Figure 4. The XPS spectrum shows the presence of emissions originating from the C1s orbital at a binding energy of 283.6 eV which indicates the presence of a C-C or C-H bond and at 286.88 eV which comes from a C-N bond. The N1s peak was observed at 399.0 eV. The peaks originating from lead are $Pb4p_{3/2}$ at 643.92 eV, $Pb4d_{5/2}$ at 412.28 eV and 434.57 eV ($4d_{3/2}$), 137.26 eV originating from $Pb4f_{7/2}$ and 142.09 eV from $Pb4f_{5/2}$. Bromide bond originating from Br1s is observed at 254.26 eV, while binding energy at 180.59 eV comes from $Br2p_{3/2}$, 187.39 eV from $Br2p_{1/2}$, $Br3d_{5/2}$ at 67.11 eV and 68.12 eV from $Br3d_{3/2}$. However, the XPS measurement showed that a peak originating from oxygen, namely the O1s orbital at 531.10 eV is clearly observed [26]. This shows that the $FAPbBr_3$ crystal has undergone an oxidation process, so that oxygen atoms enter the crystal structure. The oxygen peneteration into the crystal mighr be caused by synthesis of AVC method was conducted at room temperature with high humidity condition (above 70% relative humidity). Therefore, optimization of the synthesis process of single crystal $FAPbBr_3$ is required to minimize the penetration of oxygen atoms into the crystal. The presence of oxygen atoms will cause defects in the crystal, thus reducing the transport properties or lowering the value of lifetime-mobility product, which will ultimately deteriorate the performance of the γ-ray detector device.

## 4. Conclusions

The perovskite of formamidium-lead tribromide ($FAPbBr_3$) crystals was succesfully synthesized using the AVC method. The largest dimention of crystal is 5 mm x 5 mm x 3 mm. The XRD pattern shows domination peaks at 14.69° (100) and at 29.82° (200), which shows that the $FAPbBr_3$ crystal is a single crystal with crystal plane oriented in the x-axis direction. The crystal has an energy gap of 2.10 eV. All the constituent elements of $FAPbBr_3$ is clearly identified as confirmed by the XPS measurement. A peak at 532.1 eV originating from C=O bond caused by oxidation during synthesis is still observed. The synthesis process must be optimized to prevent oxidation into $FAPbBr_3$ single crystal, in order to produce high γ-ray detector performance.

## Acknowledgement

This research was funded by the Ministry of Research, Technology and Higher Education Indonesia, through research scheme Penelitian Fundamental Reguler (PFR), contract number 3842/UN6.3.1/PT.00/2024 dated on June 13, 2024.

## References

1. O. Baussens, G. Montémont, J. M. Verilhac, et al., Noise spectroscopy study of methylammonium lead tribromide single-crystal detectors: gamma-ray spectroscopy applications, Nucl. Instrum. Methods Phys. Res., Sect. A Vol. 1038 (2022), 166904. https://doi.org/10.1016/j.nima.2022.166904.
2. S. Yakunin, D. N. Dirin, Y. Shynkarenko, et al., Detection of gamma photons using solutiongrown single crystals of hybrid lead halide perovskites, Nat. Photonics Vol. 10(2016), 585–589M. https://doi.org/10.1038/nphoton.2016.139.
3. C. Szeles, CdZnTe and CdTe materials for X-ray and Gamma-ray radiation detector applications. Phys. Status Solidi B Vol. 241 (2004), 783−790. https://doi.org/10.1002/pssb.200304296.

4. G. I. Ayzenshtat, D. L. Budnitskii, D. Y. Mokeev, et al., Gamma-ray detectors based on GaAs<Cr> for nanostructural investigations, Russ. Phys. J. Vol 51 (2008), 1037–1052 (2008). https://doi.org/10.1007/s11182-009-9141-7.
5. L. C. Johnson, D. L. Campbell, E. L. Hull, T. E. Peterson, Characterization of a high-purity germanium detector for small-animal SPECT, Phys. Med. Biol. Vol. 56 (2011), 5877–5888. https://doi: 10.1088/0031-9155/56/18/007.
6. P. Sangsingkeow, K. D. Berry, E. J. Dumas, et al., Advances in germanium detector technology, Nucl. Instrum. Methods Phys. Res. A. Vol. 505 (2003), 183–186. https://doi.org/10.1016/S0168-9002(03)01047-7.
7. Z. Zhang, G. Yang, Recent advancements in using perovskite single crystals for gamma-ray detection, J. Mater. Sci. Mater. Electron. Vol. 32v(2021), 12758–12770. https://doi.org/10.1007/s10854-020-03519-z.
8. F. Liu, R. Wu, J. Wei, et al., Recent progress in halide perovskite radiation detectors for gamma-ray spectroscopy, ACS Energy Lett. Vol. 7 (2022), 1066−1085. https://doi.org/10.1021/acsenergylett.2c00031.
9. F. Zhang, B. Yang, K. Zheng, et al., Formamidinium lead bromide ($FAPbBr_3$) perovskite microcrystals for sensitive and fast photodetectors, Nano-Micro Lett. Vol. 10 (2018), 43. https://doi.org/10.1007/s40820-018-0196-2.
10. M. Saidaminov, V. Adinolfi, R. Comin, R. et al. Planar-integrated single-crystalline perovskite photodetectors, Nat. Commun. Vol 6 (2015), 8724. https://doi.org/10.1038/ncomms9724.
11. Y. He, W. Ke, G. C. B. Alexander et al., Resolving the energy of γ-ray photons with $MAPbI_3$ single crystals, ACS Photonics Vol. 5 (2018), 4132–4138. https://doi.org/10.1021/acsphotonics.8b00873.
12. R. M. Muslimawati, M. Manawan, K. Takahashi, Y. Furukawa, A. Bahtiar, Single crystal perovskite $MAPbBr_3$ prepared by using anti-solvent vapor-assisted crystallization method, J. Phy.: Conf. Ser. Vol. 2376 (2022), 012005. https://doi:10.1088/1742-6596/2376/1/012005.
13. G. R. Kumar, A. D. Savariraj, S. N. Karthick et al., Phase transition kinetics and surface binding states of methylammonium lead iodide perovskite, Phys. Chem. Chem. Phys., Vol. 18 (2016), 7284-7292. https://doi.org/10.1039/C5CP06232B.
14. Y. Li, F. Z. Liu, M. Waqas et al., Formamidinium-based lead halide perovskites: structure, properties, and fabrication methodologies, Small Methods Vol. 2 (2018), 1700387. https://doi.org/10.1002/smtd.201700387.
15. M. I. Saidaminov, A. L. Abdelhady, G. Maculana, O. M. Bakr, Retrograde solubility of formamidinium and methylammonium lead halide perovskites enabling rapid single crystal growth, Chem. Commun. Vol. 51 (2015), 17658-17661. https://doi.org/10.1039/C5CC06916E.
16. A. A. Zhumekenov, M. I. Saidaminov, Md. A. Haque et al., Formamidinium lead halide perovskite crystals with unprecedented long carrier dynamics and diffusion length, ACS Energy Lett. Vol. 1 (2016), 32−37. https://doi.org/10.1021/acsenergylett.6b00002.
17. X. Liu, M. Xu, Y. Hao et al., Solution-grown formamidinium hybrid perovskite ($FAPbBr_3$) single crystals for α-particle and γ-ray detection at room temperature, ACS Appl. Mater. Interfaces Vol. 13 (2021), 15383−15390. https://doi.org/10.1021/acsami.1c00174.
18. R. M. Muslimawati, M. Manawan, A. Bahtiar, Synthesis of single crystal perovskite $MAPbBr_3$ by using anti-solvent vapor-assisted crystallization method for X-ray

photodetector application, J. Phy.: Conf. Ser. Vol. 2344 (2022), 012002. https://doi:10.1088/1742-6596/2344/1/012002.
19. Y. Liu, Y. Zhang, Z. Yang et al., Inch-sized high-quality perovskite single crystals by suppressing phase segregation for light-powered integrated circuits, Sci. Adv. Vol. 7 (2021), eabc8844. https://doi:10.1126/sciadv.abc884.
20. A. D. Karabanov, A. N. Salak, C. Escobar et al., Synthesis, structure, and optical properties of large $FAPbBr_3$ perovskite single crystals, Integr. Ferroelectr. Vol. 220 (2021), 46–55. https://doi.org/10.1080/10584587.2021.1921534.
21. X. Liu, Q. Zhang, D. Zhao et al., Improved crystallization quality of $FAPbBr_3$ single crystals by a seeded solution method, ACS Appl. Mater. Interfaces Vol. 14 (2022), 51130−51136. https://doi.org/10.1021/acsami.2c15343.
22. L. Zhao, Y. Zhou, Z. Shi et al., High-yield growth of $FACsPbBr_3$ single crystals with low defect density from mixed solvents for gamma-ray spectroscopy, Nat. Photon. Vol. 17 (20234), 315–323. https://doi.org/10.1038/s41566-023-01154-8.
23. C. Li, E. J. Juarez-Perez, A. Mayora, Atomic-level understanding of a formamidinium hybrid halide perovskite, $FAPbBr_3$, Chem. Commun. Vol. 58 (2022), 12164–12167. https://doi.org/10.1039/D2CC04124C.
24. Y. Y. Pan, Y. H. Su, C. H. Hsu et al., First-principles study on electronic structures of $FAPbX_3$ (X= Cl, Br, I) hybrid perovskites, J. Adv. Nanomater. Vol. 1 (2016), 33–38. https://dx.doi.org/10.22606/jan.2016.11004.
25. F. Liu, M. Yoho, H. Tsai et al., The working principle of hybrid perovskite gamma-ray photon counter, Mater. Today Vol. 37 (2020), 27–34. https://doi.org/10.1016/j.mattod.2020.02.022.
26. K. Wang, B. R. Ecker, M. Ghosh et al., Light-enhanced oxygen degradation of $MAPbBr_3$ single crystal, Phys. Chem. Chem. Phys. Vol. 26 (2024), 5027–5037. https://doi.org/10.1039/d3cp03493c.